

Prototyping of a LQG Compensator for a Compliant Positioning System with Friction

H. Henrichfreise
Cologne Laboratory of Mechatronics
University of applied sciences Cologne
henrichfreise@kt.fh-koeln.de

Introduction

With increasing demands on speed and accuracy of positioning systems, friction and compliance which are present in every mechanical system have to be actively influenced by control. This requires to abandon the wide-spread classical (PI, PID) control concepts and apply more advanced approaches. LQG (linear quadratic Gaussian) control is one of the candidates which is capable to do active vibration damping and disturbance (friction) compensation, allowing for a high control bandwidth, strong disturbance rejection, and precise positioning with rapid changes of speed and acceleration. If properly designed and implemented, LQG control also shows a high robustness against external disturbances, nonlinear system behaviour, and plant parameter variations. Although control engineers have the theoretical background which is well explained in most control design textbooks, e.g.[1][2], one can still hear arguing against LQG control with the more demanding theory, the complex computational tasks, the difficulty to find appropriate design parameters, and the more demanding implementation issues. These arguments mostly originate from the lack of knowledge about the systematic procedure for design and implementation of LQG control, and about the extensive support given by recent development environments [3] for system modelling, analysis, design, simulation and rapid prototyping of control systems. In order to at least improve the knowledge about the procedure of LQG design and implementation, the aim of this paper is to show a straightforward approach for the position control of a compliant positioning system with friction. Since it has already been applied to other positioning devices, the approach can be seen as a sample for highly dynamical and precise position control design.

1. Compliant positioning system with friction

Figure 1 shows the structure of the electromechanical positioning system (EMPS) which is used for experimentation with position control at the Cologne Laboratory of Mechatronics (CLM).

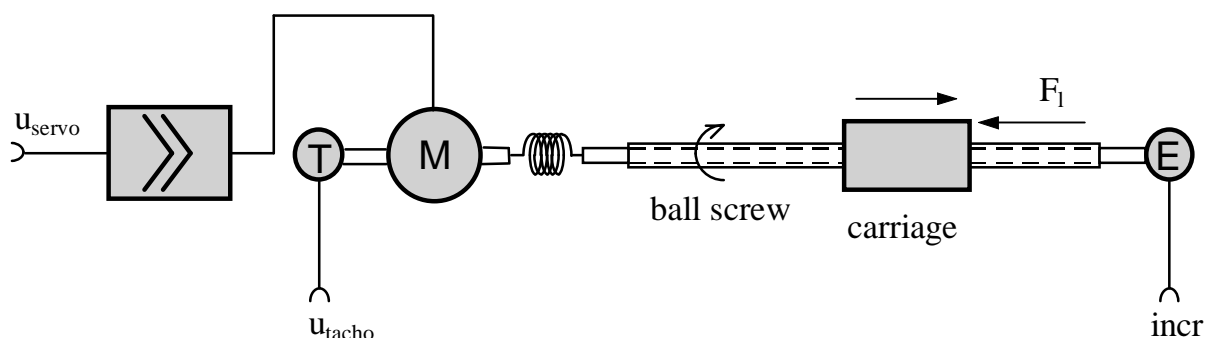


Fig. 1 Electromechanical positioning system (EMPS)

The EMPS plant consists of a DC motor with a current controlled servo amplifier and a linear positioning unit. A backlash-free ball screw drive converts the rotatory motion of the motor to the linear carriage displacement. A DC tachometer provides the velocity of the motor shaft, and an incremental encoder measures the carriage position. This is a standard configuration of drive systems in machine tools and gantry type robots. Compliance causing a mechanical resonance at about 100 Hz is added to the system by a flexible coupling between motor and positioning unit. The major source of dry friction is the ball screw drive. This friction is caused by a pre-loading of the ball screw system, which is applied to avoid backlash.

To set up a mathematical model for control design, the mechanical part of the plant is described by a two degree of freedom rotatory system. Motor and tachometer build the drive-side moment of inertia J_d , the screw, the encoder and the carriage inertias add up to J_l at the load side. The compliance between motor and positioning unit is modelled by a spring with stiffness c_{dl} and damping constant b_{dl} for material damping. Viscous friction is allocated to the drive and the load side by damping constants b_d and b_l . The dry friction in the ball screw drive is accounted for by an "internal" load-side friction torque M_{frl} . External forces F_l acting at the carriage, e.g. the cutting forces in a machine tool application, are taken care of by an extra torque input $M_l = F_l / i_s$, where i_s the gear ratio of the ball screw unit. The system is driven by the motor torque M_d . Selecting the drive-side and load-side angular displacements φ_d and φ_l as generalized coordinates, with their derivatives Ω_d and Ω_l the equations of motion for the mechanical part of the plant become

$$\begin{aligned} J_d \cdot \dot{\Omega}_d &= M_d - b_d \cdot \Omega_d - b_{dl} \cdot (\Omega_d - \Omega_l) - c_{dl} \cdot (\varphi_d - \varphi_l) \\ J_l \cdot \dot{\Omega}_l &= b_{dl} \cdot (\Omega_d - \Omega_l) + c_{dl} \cdot (\varphi_d - \varphi_l) - b_l \cdot \Omega_l - (M_l + M_{frl}) \end{aligned} \quad (1.1a)$$

A simple model used for the nonlinear dry friction including sticking, break-away and sliding friction is formulated as

$$M_{frl} = \begin{cases} M_{extl} & \text{for } \Omega_l = 0 \wedge |M_{extl}| \leq M_{Sl} \\ M_{Sl} \cdot \text{sgn}(M_{extl}) & \text{for } \Omega_l = 0 \wedge |M_{extl}| > M_{Sl} \\ M_{frl}(|\Omega_l|) \cdot \text{sgn}(\Omega_l) & \text{for } \Omega_l \neq 0 \end{cases} \quad (1.1b)$$

where

$$M_{frl}(\Omega_l) = M_{Kl} + (M_{Sl} - M_{Kl}) \cdot e^{-\frac{\Omega_l}{\Delta\Omega}} \quad , \quad \Omega_l \geq 0 \quad (1.1c)$$

is a Stribeck characteristic with the maximum static (break-away) friction M_{Sl} , the constant level of kinetic friction M_{Kl} (independent of velocity) and an exponential decay from static to kinetic friction with the constant $\Delta\Omega$, and

$$M_{extl} = c_{dl}(\varphi_d - \varphi_l) + b_{dl}(\Omega_d - \Omega_l) - b_l \Omega_l - M_l \quad (1.1d)$$

is the external torque acting at the inertia J_l .

A simple first order lag system

$$T_{servo} \dot{M}_d + M_d = k_{servo} (u_{servo} + v_{servo}) \quad (1.2)$$

with gain k_{servo} and time constant T_{servo} models the servo amplifier generating the motor torque M_d from the input voltage u_{servo} . This model also contains a disturbance input v_{servo} for servo amplifier noise.

The transducer behaviour from the motor velocity Ω_d to the tachometer voltage u_{tacho} and from the screw displacement φ_1 to the incremental encoder counter value incr are described by the equations

$$u_{\text{tacho}} = k_{\text{corr}} \cdot (k_{\Omega} \cdot \Omega_d + u_{\text{ripple}}) + \mu_{\text{tacho}} + w_{\text{tacho}} \quad (1.3a)$$

$$u_{\text{ripple}} = r_{\text{ripple}} \cdot k_{\Omega} \cdot \Omega_d \cdot \left| \sin(\varphi_d n_{\text{ripple}}) \right|$$

$$k_{\text{corr}} = \frac{1}{1 + r_{\text{ripple}} \frac{2}{\pi}}$$

$$\text{incr} = \frac{1}{2^{b_{\text{incr}}-1}} \text{trunc} \left(2^{b_{\text{incr}}-1} \cdot \frac{\varphi_1}{\varphi_{\text{max}}} \right) = q_{\text{incr}} \cdot \text{trunc} \left(\frac{1}{q_{\text{incr}}} \cdot k_{\varphi} \cdot \varphi_1 \right), \quad (1.3b)$$

where the terms $k_{\Omega}\Omega_d$ and $k_{\varphi}\varphi_1$ model the linear transducer properties. Nonlinear properties included in this model are an angular position-dependent ripple on the tachometer signal and the quantization characteristic of the incremental encoder which have to be considered for precise position control. In equation (1.3a), the factor r_{ripple} builds the ripple amplitude from the undisturbed linear signal $k_{\Omega}\Omega_d$, n_{ripple} is the number of ripples per half turn of the tachometer shaft, and the factor k_{corr} recovers the mean value of the ripple-free signal. The quantization of the incremental encoder signal in equation (1.3b) is given by the integer number of bits b_{incr} required to cover the angular position range of $\pm\varphi_{\text{max}}$, where q_{incr} is the quantization step size for a range ± 1 of the counter value incr . Other measurement disturbances are the offset voltage μ_{tacho} and noise w_{tacho} on the tachometer signal.

Equations (1.1) to (1.3) have been transformed to a SIMULINK block diagram for simulation of the nonlinear control system with the LQG compensator described in the following section.

The linear plant model needed for compensator design has been derived by dropping the nonlinear terms and the servo amplifier and measurement disturbances in the above equations. Choosing the angular velocities, positions, and the motor torque as state variables, the state space equations of the linear plant model with the state differential equation and measurement output equation become

$$\dot{\underline{x}}_p = \underline{A}_p \underline{x}_p + \underline{B}_{pc} \underline{u}_{pc} + \underline{B}_{pd} \underline{u}_{pd}$$

$$\begin{bmatrix} \dot{\varphi}_d \\ \dot{\Omega}_d \\ \dot{\varphi}_1 \\ \dot{\Omega}_1 \\ \dot{M}_d \end{bmatrix} = \begin{bmatrix} 0 & 1 & 0 & 0 & 0 \\ -\frac{c_{dl}}{J_d} & -\frac{b_d + b_{dl}}{J_d} & \frac{c_{dl}}{J_d} & \frac{b_{dl}}{J_d} & \frac{1}{J_d} \\ 0 & 0 & 0 & 1 & 0 \\ \frac{c_{dl}}{J_1} & \frac{b_{dl}}{J_1} & -\frac{c_{dl}}{J_1} & -\frac{b_{dl} + b_{l1}}{J_1} & 0 \\ 0 & 0 & 0 & 0 & -\frac{1}{T_{servo}} \end{bmatrix} \cdot \begin{bmatrix} \varphi_d \\ \Omega_d \\ \varphi_1 \\ \Omega_1 \\ M_d \end{bmatrix} + \begin{bmatrix} 0 \\ 0 \\ 0 \\ 0 \\ \frac{k_{servo}}{T_{servo}} \end{bmatrix} \cdot \underline{u}_{servo} + \begin{bmatrix} 0 \\ 0 \\ 0 \\ \frac{1}{J_1} \\ 0 \end{bmatrix} \cdot (M_1 + M_{fr}) \quad (1.4a)$$

$$\underline{y}_{pm} = \underline{C}_{pm} \underline{x}_p$$

$$\begin{bmatrix} \underline{u}_{tacho} \\ \underline{incr} \end{bmatrix} = \begin{bmatrix} 0 & k_{\Omega} & 0 & 0 & 0 \\ 0 & 0 & k_{\varphi} & 0 & 0 \end{bmatrix} \cdot \begin{bmatrix} \varphi_d \\ \Omega_d \\ \varphi_1 \\ \Omega_1 \\ M_d \end{bmatrix} \quad (1.4b)$$

Another equation needed for compensator design is the output equation

$$\underline{y}_{po} = \underline{C}_{po} \underline{x}_p + \underline{D}_{pod} \underline{u}_{pd} \quad (1.4c)$$

$$\begin{bmatrix} \varphi_1 \\ \Omega_1 \\ \alpha_1 \end{bmatrix} = \begin{bmatrix} 0 & 0 & 1 & 0 & 0 \\ 0 & 0 & 0 & 1 & 0 \\ \frac{c_{dl}}{J_1} & \frac{b_{dl}}{J_1} & -\frac{c_{dl}}{J_1} & -\frac{b_{dl} + b_{l1}}{J_1} & 0 \end{bmatrix} \cdot \begin{bmatrix} \varphi_d \\ \Omega_d \\ \varphi_1 \\ \Omega_1 \\ M_d \end{bmatrix} + \begin{bmatrix} 0 \\ 0 \\ -\frac{1}{J_1} \end{bmatrix} \cdot (M_1 + M_{fr})$$

for the objective variables of the plant, the load-side angular position φ_1 , velocity Ω_1 , and acceleration $\alpha_1 = \dot{\Omega}_1$, which will be used to formulate the design objectives for the carriage motion.

The subscripts p, c, d, m, o at the above vectors and matrices stand for plant, control, disturbance, measurement and objective, respectively.

The above equations are the basis for the design and closed-loop simulation of a LQG compensator which shall provide excellent reference profile tracking in the presence of disturbances from noise, external loads and internal friction. The corresponding linear and nonlinear model parameters which are needed for the numerical evaluations have been properly identified in [4]. A more comprehensive model with a detailed nonlinear modelling of the servo

amplifier, load dependency and delayed friction in the friction model, and additional drive-side friction is used in [5], which is however not required in the context of this paper.

2. LQG design

Different types of controllers have been designed for the EMPS, from a simple PID controller up to an output vector feedback with observer-based friction compensation [5][6]. The topic of this paper is the design and implementation of a steady-state LQG dynamic regulator (compensator) for the linear plant model from equations (1.4). To include effects from the real environment, these equations are augmented by suitable linear models for reference and disturbance excitation. A weighting model is added to take into account engineering objectives in the design process. This approach and reasonable design parameters lets the compensator outperform all the above mentioned control structures. The LQG compensator will be designed following the separation principle: First a linear quadratic regulator (LQR) is designed for steady-state reference tracking and disturbance rejection, then a linear quadratic observer (LQE) is added to provide the states which are not measurable.

2.1 LQR design

To include the design objectives and the operational environment of the plant in the design process, equations (1.4a) and (1.4c) are taken for the linear plant model and are augmented by a weighting model

$$\begin{aligned} \dot{\underline{x}}_w &= \underline{A}_w \underline{x}_w + \underline{B}_{wr} \underline{u}_{wr} + \underline{B}_{wp} \underline{u}_{wp}, & \underline{x}_w(t=0) &= \underline{0} \\ \underline{y}_w &= \underline{C}_w \underline{x}_w + \underline{D}_{wr} \underline{u}_{wr} + \underline{D}_{wp} \underline{u}_{wp} \end{aligned}, \quad (2.1a)$$

a reference excitation model

$$\begin{aligned} \dot{\underline{x}}_r &= \underline{A}_r \underline{x}_r, & \underline{x}_r(t=0) &= \underline{x}_{r0} \\ \underline{y}_r &= \underline{C}_r \underline{x}_r \end{aligned}, \quad (2.1b)$$

and a disturbance excitation model

$$\begin{aligned} \dot{\underline{x}}_d &= \underline{A}_d \underline{x}_d, & \underline{x}_d(t=0) &= \underline{x}_{d0} \\ \underline{y}_d &= \underline{C}_d \underline{x}_d \end{aligned} \quad (2.1c)$$

as shown in figure 2.

With the above models, as under real world conditions, the plant is considered to work in a mixed deterministic and stochastic environment [7].

The deterministic environment of the plant is given by all signals whose shapes are known, but whose amplitudes can only be specified for a certain experiment. In figure 2 these signals are the reference and disturbance signals \underline{u}_{wr} and \underline{u}_{pd} which are generated by the reference and disturbance models from appropriate initial conditions \underline{x}_{r0} and \underline{x}_{d0} of their states. To cover all possible experiments including varying initial conditions for the plant states, the initial conditions \underline{x}_{r0} , \underline{x}_{d0} and \underline{x}_{p0} are assumed to be unknown random variables with zero mean, given variances and a Gaussian distribution. With this deterministic environment it is easy to find appropriate model dynamics to generate the classes of time functions appearing under real

operating conditions [7]. The fact that only their shapes have deterministic character while their amplitudes are random variables implies that the controlled system shall work for any meaningful amplitudes (initial conditions) and not only accurately track a single reference or reject a single disturbance torque profile.

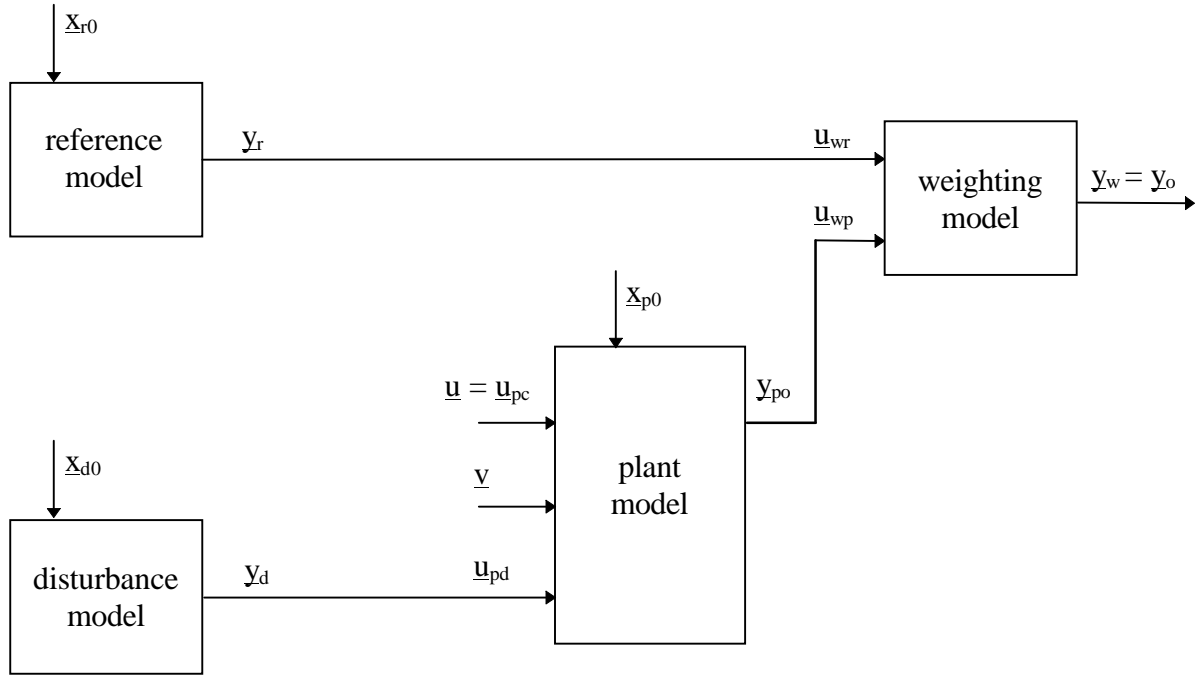


Fig. 2 Augmented plant model for LQR design

In the following, the models for position control of the EMPS will be discussed.

A triple pseudo integrator

$$\dot{\underline{x}}_r = \begin{bmatrix} -\frac{1}{T_r} & 1 & 0 \\ 0 & -\frac{1}{T_r} & 1 \\ 0 & 0 & -\frac{1}{T_r} \end{bmatrix} \underline{x}_r, \quad \underline{x}_r = \begin{bmatrix} \phi_r \\ \Omega_r \\ \alpha_r \end{bmatrix}, \quad \underline{x}_r(t=0) = \underline{x}_{r0} \quad (2.2a)$$

$$\underline{y}_r = \begin{bmatrix} 1 & 0 & 0 \\ 0 & 1 & 0 \\ 0 & 0 & 1 \end{bmatrix} \underline{x}_r$$

is appropriate to generate step, ramp, and parabolic position reference signals and their first and second derivatives for the elements of the output vector \underline{y}_r . With $T_r \rightarrow \infty$ tending to a true triple integrator, it provides the same type of output time functions from the initial conditions in the vector \underline{x}_{r0} as the reference profile generator in the final implementation of the control system.

If the disturbing torques at the plant input $u_{pd} = (M_l + M_{fr})$ are assumed to be step functions, which exactly models kinetic friction for $M_S = M_K$ in equations (1.1b)-(1.1d) and constant external loads, the disturbance model becomes the single pseudo integrator

$$\dot{x}_d = -\frac{1}{T_d} x_d, \quad x_d(t=0) = x_{d0} \quad (2.2b)$$

$$y_d = x_d$$

which approaches a true integrator where $T_d \rightarrow \infty$.

The need of pseudo integrators is imposed by the condition that the integral cost function for LQR design requires a finite value, i.e. stable time responses of the contributing state variables for given initial conditions¹. Because the above excitation model states are not controllable from the system input $\underline{u} = \underline{u}_{pc} = \underline{u}_{servo}$ (see figure 2) and hence cannot be stabilized by feedback, their integral behaviour must be approximated by very slow first order systems which are called pseudo integrators. Their time constants have to be chosen far beyond the desired time constants in the closed-loop transient response. The results achieved from this approximation are numerically identical to those from the theoretical exact approach [8].

With the above definition of the deterministic environment, the stochastic environment of the plant is the remaining rest of all signals whose shapes and amplitudes are unknown. If nothing is known about their spectral properties, these signals can be modelled as a zero-mean, Gaussian white noise vector process \underline{v} with constant intensity matrix \underline{V} disturbing the plant state variables (see figure 2). Otherwise the respective signals could be modelled from white noise processes by the use of an appropriate linear filter model which then as a disturbance model also becomes part of the augmented plant model. With the inclusion of this stochastic environment to the design process it becomes clear that the LQR will be rejective to unknown disturbances and, to some extent, even to parameter variations in the real system. This rejectiveness is achieved with the design in the way that the influence of the disturbance signals to the LQR cost functions (see below) and thus to the corresponding controlled system time responses will be kept as small as possible with respect to the given design constraints, e.g. a limited control signal range.

Besides the modelling of the system excitation, the other issue addressed in figure 2 is the formulation of engineering objectives. The weighting model

$$\underline{y}_w = \begin{bmatrix} e_\phi \\ e_\Omega \\ e_\alpha \end{bmatrix} = \begin{bmatrix} 1 & 0 & 0 \\ 0 & 1 & 0 \\ 0 & 0 & 1 \end{bmatrix} \underline{u}_{wr} + \begin{bmatrix} -1 & 0 & 0 \\ 0 & -1 & 0 \\ 0 & 0 & -1 \end{bmatrix} \underline{u}_{wp} \quad (2.2c)$$

is used to build the design objective variables for the output vector \underline{y}_o of the augmented plant model. They are subject to the LQR design procedure. By using the errors e_ϕ , e_Ω , and e_α of the load-side angular position, velocity and acceleration from the desired variables in the reference model output vector \underline{y}_r , the LQR design will yield steady-state accuracy for the considered class of reference and disturbance excitation by feedforward of the respective reference and disturbance model states.

Since it does not contain a state differential equation and does not contribute a state to the augmented plant model, the weighting model from equation (2.2c) performs a purely proportional weighting. With integral weighting of the position error the weighting model would look like

¹ For white noise excitation the integrand of the LQR cost function must become stationary.

$$\dot{\underline{x}}_w = 0 \underline{x}_w + [1 \ 0 \ 0] \underline{u}_{wr} + [-1 \ 0 \ 0] \underline{u}_{wp}, \quad \underline{x}_w(t=0) = 0$$

$$\underline{y}_w = \begin{bmatrix} e_\phi \\ e_\Omega \\ e_\alpha \\ x_w \end{bmatrix} = \begin{bmatrix} 0 \\ 0 \\ 0 \\ 1 \end{bmatrix} \underline{x}_w + \begin{bmatrix} 1 & 0 & 0 \\ 0 & 1 & 0 \\ 0 & 0 & 1 \\ 0 & 0 & 0 \end{bmatrix} \underline{u}_{wr} + \begin{bmatrix} -1 & 0 & 0 \\ 0 & -1 & 0 \\ 0 & 0 & -1 \\ 0 & 0 & 0 \end{bmatrix} \underline{u}_{wp} \quad (2.2d)$$

which has been investigated for the EMPS position control in [9]. Feedback of the state \underline{x}_w from the LQR design yields an integral state feedback which is capable to produce steady-state accuracy for a constant disturbance signal at the plant input \underline{u}_{pd} . Integral feedback is suitable for steady-state errors whose sources are not well known or are not easy to model, or which can not be compensated by other means. For the compensation of steady-state errors due to friction and external torques the disturbance model and resulting state feedforward is preferable. Additional integral feedback may be useful if remaining errors are of the above mentioned type. Since for the EMPS the better results have been achieved with the disturbance model (2.2b) and the proportional weighting from equation (2.2c), this approach has been followed up in this paper.

By substitution of the input and output variables corresponding to figure 2, the above models can easily be combined to the state differential and objective output equation

$$\dot{\underline{x}} = \underline{A} \underline{x} + \underline{B} \underline{u} + \underline{F} \underline{v}, \quad \underline{x}(t=0) = \underline{x}_0$$

$$\underline{y}_o = \underline{C} \underline{x} \quad (2.3a)$$

of the augmented plant model for LQR design [5], where for the general case

$$\underline{x} = \begin{bmatrix} \underline{x}_p \\ \underline{x}_r \\ \underline{x}_d \\ \underline{x}_w \end{bmatrix}, \quad \underline{u} = \underline{u}_{pc}, \quad \underline{y}_o = \underline{y}_w$$

$$\underline{A} = \begin{bmatrix} \underline{A}_p & \underline{0} & \underline{B}_{pd} \underline{C}_d & \underline{0} \\ \underline{0} & \underline{A}_r & \underline{0} & \underline{0} \\ \underline{0} & \underline{0} & \underline{A}_d & \underline{0} \\ \underline{B}_{wp} \underline{C}_{po} & \underline{B}_{wr} \underline{C}_r & \underline{B}_{wp} \underline{D}_{pod} \underline{C}_d & \underline{A}_w \end{bmatrix}, \quad \underline{B} = \begin{bmatrix} \underline{B}_{pc} \\ \underline{0} \\ \underline{0} \\ \underline{0} \end{bmatrix}, \quad \underline{F} = \begin{bmatrix} \underline{F}_p \\ \underline{0} \\ \underline{0} \\ \underline{0} \end{bmatrix}$$

and

$$\underline{C} = [\underline{D}_{wp} \underline{C}_{po} \quad \underline{D}_{wr} \underline{C}_r \quad \underline{D}_{wp} \underline{D}_{pod} \underline{C}_d \quad \underline{C}_w]. \quad (2.3b)$$

LQR design for this model provides the gain matrix \underline{K} for the optimal linear regulator

$$\underline{u} = -\underline{K} \cdot \underline{x} = -[\underline{K}_p \quad \underline{K}_r \quad \underline{K}_d \quad \underline{K}_w] \cdot \begin{bmatrix} \underline{x}_p \\ \underline{x}_r \\ \underline{x}_d \\ \underline{x}_w \end{bmatrix} \quad (2.4)$$

including feedforward of the reference and disturbance model states by the gain submatrices \underline{K}_r and \underline{K}_d , and feedback of the plant and weighting model states by the matrices \underline{K}_p and \underline{K}_w . While the feedforward provides steady-state accuracy for the given classes of reference and disturbance signals, the feedback of the plant and weighting model states stabilizes unstable modes and produces a fast and well damped decay of the remaining transient and steady-state errors around the reference time profiles.

The optimal regulator minimizes the quadratic cost functions (2.5a) and (2.5b) built by the weighted engineering objectives from the output vector \underline{y}_o and by the weighted control input \underline{u} . They are the expected value of the steady-state ($t \rightarrow \infty$) integral

$$J = E\left\{\lim_{t \rightarrow \infty} \int_0^t \left(\underline{y}_o^T \underline{Q} \underline{y}_o + \underline{u}^T \underline{R} \underline{u} \right) d\tau\right\} \quad (2.5a)$$

for the system excited from the deterministic environment, or the steady-state expected value

$$J = \lim_{t \rightarrow \infty} E\left\{ \underline{y}_o^T \underline{Q} \underline{y}_o + \underline{u}^T \underline{R} \underline{u} \right\} \quad (2.5b)$$

of the integrand itself for excitation from the stochastic environment, where the symmetric weighting matrices \underline{Q} and \underline{R} have to be positive semi-definite and positive definite, respectively. With diagonal weighting matrices, the actual objective variables for proportional weighting from (2.2c) and the control input u_{servo} the quadratic forms in the above cost functions write

$$\underline{y}_o^T \underline{Q} \underline{y}_o + \underline{u}^T \underline{R} \underline{u} = q_{e_\phi} e_\phi^2 + q_{e_\Omega} e_\Omega^2 + q_{e_\alpha} e_\alpha^2 + r_{u_{\text{servo}}} u_{\text{servo}}^2 \quad (2.5c)$$

Consequently, the first cost function can be interpreted as the expected value of the weighted sum of the mean square amplitudes of the variables for random initial conditions (only factor $1/t$ before the integral is missing), the second function represents the weighted sum of the steady-state covariances for noise excitation.

It makes no difference for the result of the LQR design which case of environment and corresponding cost function is considered. For both cases [1][7] the optimal gain matrix is given by

$$\underline{K} = \underline{R}^{-1} \underline{B}^T \underline{S} \quad (2.5d)$$

where the matrix \underline{S} is the solution of the control algebraic Riccati equation

$$\underline{S} \underline{A} + \underline{A}^T \underline{S} - \underline{S} \underline{B} \underline{R}^{-1} \underline{B}^T \underline{S} + \underline{C}^T \underline{Q} \underline{C} = \underline{0} \quad (2.5e)$$

for the augmented plant model (2.3). Since the gain matrix and thus the optimal regulator does neither depend on the noise injection matrix \underline{F} nor on the intensity matrix \underline{V} of the white noise process \underline{v} in equation (2.3), the control is optimal for any noise excitation \underline{v} of the augmented plant model states. The LQR design task given by equations (2.5d) and (2.5e) can be solved with the MATLAB Control System Toolbox [10]. Due to the linearly dependent eigenvectors associated with the pseudo integrator eigenvalues in the reference model, a function basing on a Schur algorithm [11] has to be used and modified for the cost function with weighted outputs.

The design parameters still missing for evaluating the optimal gain matrix are the weightings q_{e_ϕ} , q_{e_Ω} , q_{e_α} and $r_{u_{\text{servo}}}$, which for deterministic excitation tune the controlled system behaviour by penalizing large amplitudes and slow decay of the objective variables and too extensive use of the control signal. How can suitable, physically meaningful values be determined?

If the quadratic terms in (2.5c) are interpreted as variance contributions of the individual time functions to the final cost J , one can find that the reciprocal values of the maximum allowed variances σ_i^2 for the individual signals are suitable weighting values. Applied to (2.5c) the quadratic forms write

$$\underline{y}_o^T \underline{Q} \underline{y}_o + \underline{u}^T \underline{R} \underline{u} = \frac{1}{\sigma_{e_\phi}^2} e_\phi^2 + \frac{1}{\sigma_{e_\Omega}^2} e_\Omega^2 + \frac{1}{\sigma_{e_\alpha}^2} e_\alpha^2 + \frac{1}{\sigma_{u_{\text{servo}}}^2} u_{\text{servo}}^2, \quad (2.6)$$

from which it is clear that the smaller a maximum allowed variance the higher the corresponding weighting, i.e. the penalty on the variance contribution of the respective signal to the final cost value. Because the random variables from the design environment are assumed to be Gaussianly (normally) distributed, this is also valid for the input and output signals (u_{servo} , e_ϕ , e_Ω and e_α) of the augmented plant model. For zero mean values this implies that their ranges are covered to approximately 99% by three times the individual standard deviations σ_i . Therefore the values σ_i for the weightings in (2.6) can be set to one third of the maximum allowed absolute signal values. The resulting weightings $1/\sigma_i^2$ scale the values and units of the variance contributions to (2.6) for the given constraints on the corresponding time functions. For example, if the control signal u_{servo} has a range of ± 10 V, the range of the rigid body acceleration of the EMPS is ± 15000 rad/sec², and the position error e_ϕ shall stay in a range of ± 0.15 rad (± 60 μm), the respective weightings become

$$r_{u_{\text{servo}}} = 0.09 / \text{V}^2, \quad q_{e_\alpha} = 0.0002 \text{ sec}^4 / \text{rad}^2, \quad q_{e_\phi} = 400 / \text{rad}^2.$$

Following the above rule for the weightings of the cost functions (2.5a) and (2.5b), the LQR design for the EMPS provides nice time responses right from the design start. Minor fine-tuning of the output weightings is necessary when adding the observer for the missing state variables after the second design step in order to improve the final closed-loop system time responses with the compensator.

After having found the LQR gain matrix, one has to consider that not all state variables from the augmented plant model in figure 2 can be measured or computed from feedforward commands. The only signals available are the state variables of the reference model, which can be taken from the reference profile generator as a standard part of every position control application, and the states of the weighting model, which can be computed from the model inputs and given weighting model dynamics (see section 2.3). An observer is required for the plant and disturbance model states. Indeed, the plant state variables Ω_d and ϕ_l could be computed from the measurement variables (equation (1.4b)), but they are affected by quantization and noise, and need some filtering by the observer.

LQE design of an observer to provide smooth and optimum estimates for the missing plant and disturbance model states is the topic of the next, second design step.

2.2 LQE design

The linear plant model with measurement output equation from equations (1.4a) and (1.4b) is needed for the observer design. The linear disturbance model

$$\begin{aligned} \dot{\underline{x}}_d &= \underline{A}_d \underline{x}_d + \underline{B}_d \underline{u}_d, \quad \underline{x}_d(t=0) = \underline{0} \\ \underline{y}_d &= \underline{C}_d \underline{x}_d \end{aligned} \quad (2.7a)$$

with unknown input \underline{u}_d is added as shown in figure 3 to include the deterministic disturbance environment in the observer. As already discussed for the LQR design, an integrator model

$$\begin{aligned} \dot{x}_d &= u_d, \quad x_d(t=0) = 0 \\ y_d &= x_d \end{aligned} \quad (2.7b)$$

is suitable to generate step-shaped disturbance signals for the disturbance input $u_{pd} = (M_1 + M_{fri})$ of the EMPS. One can assume Dirac pulses with random pulse weight at the disturbance model input u_d to get step-shaped outputs y_d , which is equivalent to the initial conditions for the disturbance state used for the LQR design. The fact that this deterministic input can not be measured like the other input and output signals from figure 3 will be accounted for when specifying the corresponding intensity v_d for observer design. Contrarily to the LQR design, there will be no problem with the pure integrator for the LQE design, if the disturbance model state in the augmented plant model is observable and controllable (see below).

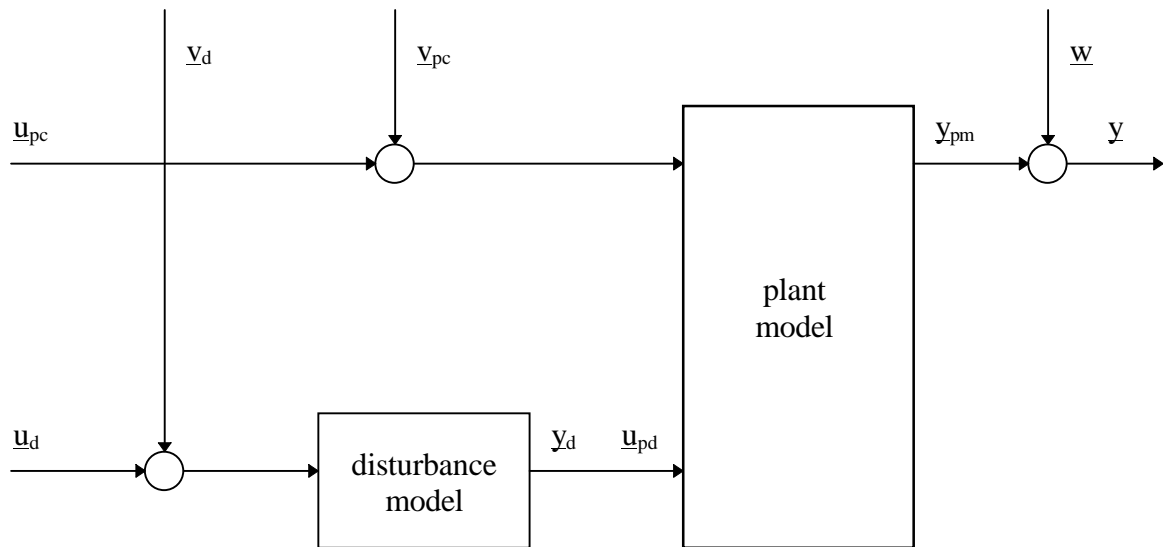


Fig. 3 Augmented plant model for LQE design

The stochastic environment of the plant model is given by the input noise vector process (process noise vector) \underline{v} and measurement noise vector process \underline{w} .

By substitution of the input and output signals and adding the noise processes corresponding to figure 3, the augmented plant model for the LQE design writes [5]

$$\begin{aligned} \dot{\underline{x}} &= \underline{A} \underline{x} + \underline{B} \underline{u} + \underline{B} \underline{v} \\ \underline{y} &= \underline{y}_{pm} + \underline{w} = \underline{C} \underline{x} + \underline{w} \end{aligned} \quad (2.8a)$$

where

$$\underline{x} = \begin{bmatrix} \underline{x}_p \\ \underline{x}_d \end{bmatrix}, \quad \underline{u} = \begin{bmatrix} \underline{u}_{pc} \\ \underline{u}_d \end{bmatrix}, \quad \underline{v} = \begin{bmatrix} \underline{v}_{pc} \\ \underline{v}_d \end{bmatrix}$$

$$\underline{A} = \begin{bmatrix} \underline{A}_p & \underline{B}_{pd} & \underline{C}_d \\ \underline{0} & \underline{A}_d & \underline{0} \end{bmatrix}, \quad \underline{B} = \begin{bmatrix} \underline{B}_{pc} & \underline{0} \\ \underline{0} & \underline{B}_d \end{bmatrix} \quad \text{and} \quad \underline{C} = \begin{bmatrix} \underline{C}_{pm} & \underline{0} \end{bmatrix}. \quad (2.8b)$$

It is required for LQE design that all states are observable in the disturbed measurement output vector \underline{y} and controllable by the augmented system input vector \underline{u} .

Injection of the process noise vector \underline{v} by the same input matrix \underline{B} as used for the input vector \underline{u} , i.e. directly at the augmented plant model input, is in preparation for trying to achieve input loop transfer recovery with the observer design.

Considering figure 4 the objective of the LQE design becomes particular clear: Find the best estimates for the noisy or unknown state variables of the plant and for the unknown disturbance model states contained in the augmented plant state vector \underline{x} in the presence of process and measurement noise. Consequently, for a high level of process noise \underline{v} and a low level of measurement noise \underline{w} , the estimator has rather to rely on the measurements than on the input signals and vice versa.

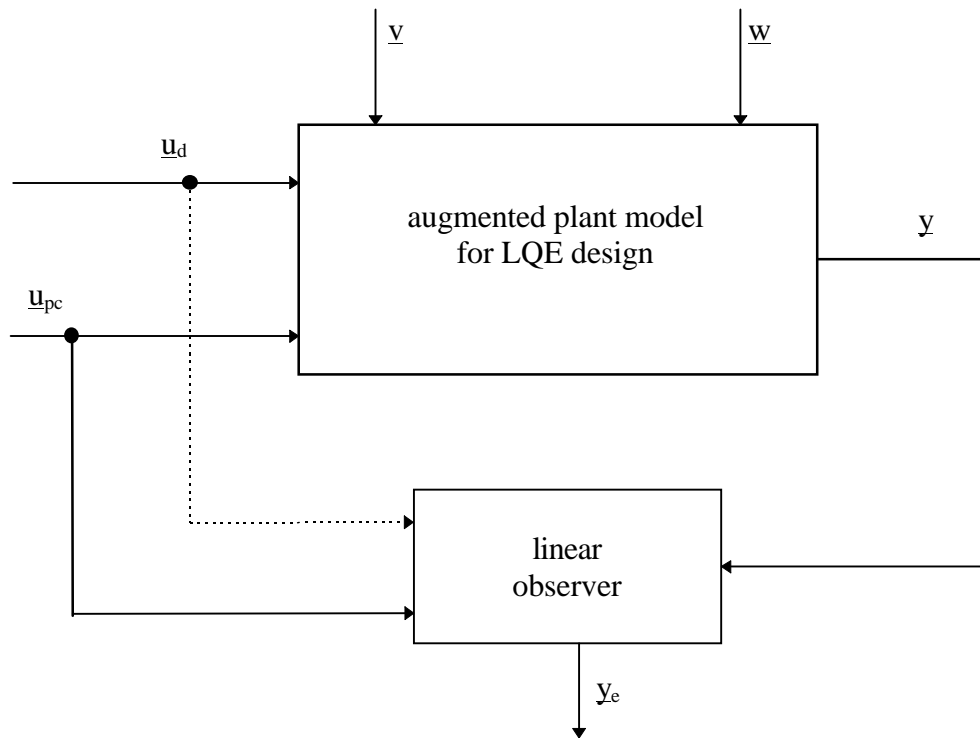


Fig. 4 Augmented plant model with linear observer

If the vector processes \underline{v} for the process noise and \underline{w} for the measurement noise are assumed to be stationary, zero-mean, Gaussian white noise processes with known constant symmetric intensity (spectral density) matrices \underline{V} and \underline{W} , the optimal observer for the augmented plant model (2.8) is given by the linear state space equations

$$\begin{aligned}\dot{\underline{x}}_e &= (\underline{A} - \underline{L}\underline{C})\underline{x}_e + \underline{B}_e \underline{u}_{pc} + \underline{L}\underline{y} \\ \underline{y}_e &= \underline{x}_e\end{aligned}\quad (2.9)$$

where \underline{B}_e ist the left hyper-column of \underline{B} from equation (2.8b).

This optimal observer minimizes the cost function

$$J = \lim_{t \rightarrow \infty} E \left\{ (\underline{x} - \underline{x}_e)^T (\underline{x} - \underline{x}_e) \right\} \quad (2.10a)$$

for the estimation error $(\underline{x} - \underline{x}_e)$, i.e. the sum of the steady-state ($t \rightarrow \infty$) autocovariances of the estimation error. LQE design for the augmented plant model provides the optimal observer gain matrix

$$\underline{L} = \underline{P}\underline{C}^T \underline{W}^{-1} \quad , \quad (2.10b)$$

where the optimal steady-state covariance matrix \underline{P} of the estimation error is the solution of the observer algebraic Riccati equation

$$\underline{A}\underline{P} + \underline{P}\underline{A}^T - \underline{P}\underline{C}^T \underline{W}^{-1} \underline{C}\underline{P} + \underline{B}\underline{V}\underline{B}^T = \underline{0} \quad . \quad (2.10c)$$

The design task given by equations (2.10b) and (2.10c) can be easily solved by using the corresponding function from MATLAB Control System Toolbox.

Meaningful intensity matrices \underline{V} and \underline{W} are needed as the design parameters for the LQE design to compute the estimator gain matrix. These matrices have a similar meaning as the weighting matrices from the LQR design, because they penalize the usage of the augmented plant inputs and measurement outputs for the estimation of the augmented state vector \underline{x} (see figure 3). The task to specify numerical values for the intensity matrices simplifies if the individual elements of the vector processes \underline{v} and \underline{w} are assumed to be uncorrelated, so that the intensity matrices $\underline{V} = \text{diag} (V_{ii})$ and $\underline{W} = \text{diag} (W_{ii})$ become diagonal.

With a closer look at the signals, as they will be seen by the observer in the later digital implementation, one can derive a simple rule to specify values for the remaining diagonal elements. We consider that all measurement signals are sampled with a sampling period T_s and, if they are not already digital like the encoder signal, are converted to digital by A/D-converters. Since the A/D-converters and the encoder have a limited resolution (wordlength or number of lines), the values at the sampling instants are subject to quantization. The resulting errors can be modelled as uniformly distributed discrete white noise processes [12] to be added to the sampled measurement signals. This so-called quantization noise has a variance of

$$\begin{aligned}\sigma_i^2 &= \frac{1}{12} \cdot \Delta_i^2 = \frac{1}{3} \cdot 2^{-2b_i} \cdot A_i^2 \quad , \\ A_i &= 2^{b_i-1} \cdot \Delta_i\end{aligned}\quad (2.11a)$$

where Δ_i is the quantization stepsize, b_i the wordlength and $\pm A_i$ the analog range of the converter. Since it is discrete white noise, the spectral density function $S_i(\omega)$ of the quantization noise has a constant intensity of σ_i^2 and is defined in the frequency range of $\pm\pi/T_s$. The discrete white noise approaches the continuous white noise spectral density function in the limit as T_s approaches zero, if σ_i^2 is set to W_{ii}/T_s [2].

Thus, if quantization noise is the only noise source for the measurement signals, which is the case for the encoder signal, suitable values for intensities of the continuous white noise processes for the LQE design are

$$W_{ii} = \sigma_i^2 T_s \quad . \quad (2.11b)$$

Since a common factor in the intensities does not affect the result of LQE design, there is no need to decide on a sampling period in this stage of the design, and the LQE design parameters can be set $W_{ii} = \sigma_i^2$.

Following the above rule, the noise intensity for the incremental encoder signal, with 17 bits needed to cover the full position range which is scaled to ± 1 , calculates $W_{22} = \sigma_{incr}^2 = 1.94 \cdot 10^{-11}$. Measurement noise not resulting from quantization (e.g. from the measurement transducers and amplifiers) can be taken into account by an equivalent quantization noise process, i.e. by decreasing the converter wordlength to an effective number of bits $b = b_{eff}$ which could be calculated from (2.11a) with a real noise variance measurement. Of course a variance measurement could directly be used as a design parameter instead.

A quick way to plug in suitable values for the design parameters is to set the quantization stepsize Δ to the range of the measured signal noise floor and use equation (2.11a) for the variance. With a noise floor of $\pm 0.01V$ on the tacho signal, Δ_{tacho} becomes $0.02V$, which results in $W_{11} = \sigma_{tacho}^2 = 3.33 \cdot 10^{-5} V^2$. This value corresponds to a effective number of bits of about 10.

A first guess for the intensity of the input noise process at the plant control input which is driven by the compensator D/A-converter output can also be found according to equation (2.11a). Again, noise not resulting from D/A-quantization (e.g. from the servo amplifier) can be taken into account by appropriately setting the quantization stepsize. The resulting variance value needs additional increase to improve the robustness of the closed-loop system with the observer by trying to achieve input loop transfer recovery (LTR) [13][2][1].

With increasing input noise intensity, the eigenvalues of the estimator tend to the transmission zeros of the augmented plant model (2.8) and to infinity. Thus the intensity is limited due to the estimator eigenvalues becoming too fast for implementation or tending to transmission zeros in the right half of the s-plane. The limiting matter for the EMPS is a transmission zero of (2.8) in the s-plane origin. If the control input noise intensity for LTR is selected too high, the eigenvalue tending to zero leads to an unsatisfying disturbance behaviour. This becomes visible by a very slow mode in the time response of the closed-loop system for a step at the disturbance input M_1 of the plant.

Since the disturbance input \underline{u}_d of the augmented plant model is unknown and can not be measured, the intensity of the corresponding noise process has to be selected as high as possible to make the estimator robust against the fact that the signal is missing for implementation. Again implementation constraints determine the intensity limits: The frequencies of the observer eigenvalues should be kept about three to ten times below the implementation sampling frequency $f_s = 1/T_s$ of the compensator.

After having discussed the proper selection of the noise intensities as LQE design parameters, let's have a closer look on the meaning of input loop transfer recovery with the illustration given in figure 5. If the control loop is cut directly before the plant input, the observer will receive a wrong input (compensator output instead of plant input). If the compensator is poorly designed, it may even become unstable due to the feedback of its output to the observer input. To achieve both robustness to a wrong input and stability, the observer has to be designed in such away that it does not need the plant control input or at least is not overly

dependent on it. This is achieved by increasing the intensity of the control input noise in the observer design. As the intensity of the control input noise is tending towards infinity, the compensator output is no longer needed as an observer input. The augmented plant state vector \underline{x} is solely reconstructed from the plant measurement output y_{pm} , so that the observer inverts the measurement output equation of the plant. If this observer is assumed to be shifted to the plant subsystem, it can be recognized that the open-loop transfer from the plant control input \underline{u}_{pc} to the LQG compensator output y_{LQG} recovers the loop transfer (LTR) from \underline{u}_{pc} to the static state feedback regulator output y_{LQR} . This also recovers the very good robustness properties with infinite gain margin and at least 60 degrees phase margin [2] of the control system with LQR, i.e. static state feedback only. For the considered transfer path the estimator dynamics are no longer of significance.

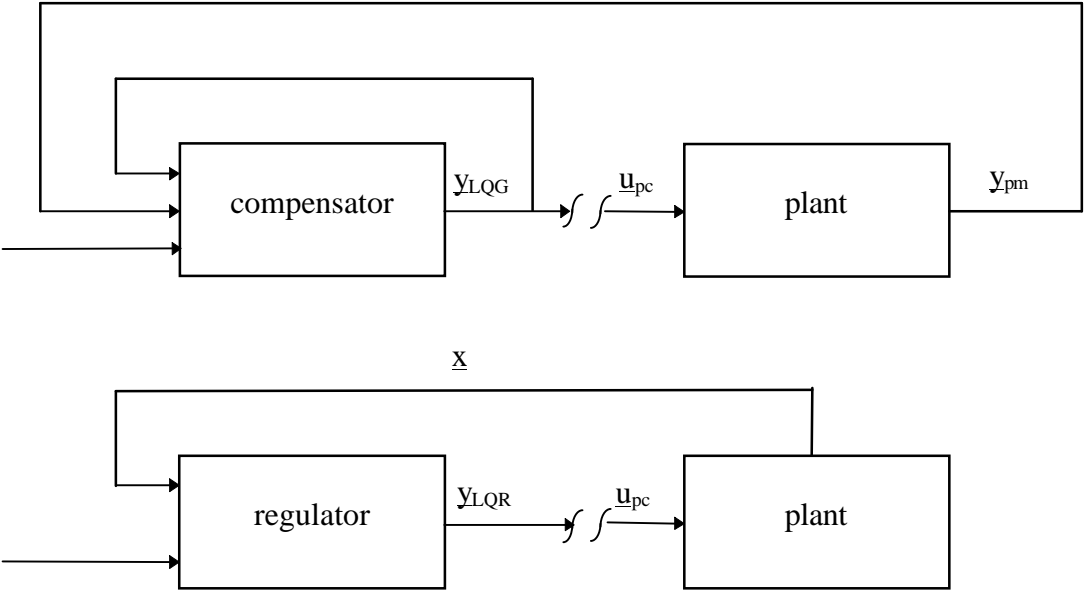


Fig. 5 *Meaning of LTR*

For a single control input to the plant the grade of LTR can be easily assessed by comparing the open-loop bode plots of the systems from figure 5. Singular value bode plots are required for multiple control inputs. They can be computed with a function from the MATLAB Control System Toolbox.

2.3 Assembly of LQG compensator

After the design of the optimal regulator and optimal observer as described in the previous sections the LQG compensator can now be assembled as shown in figure 6 and 7.

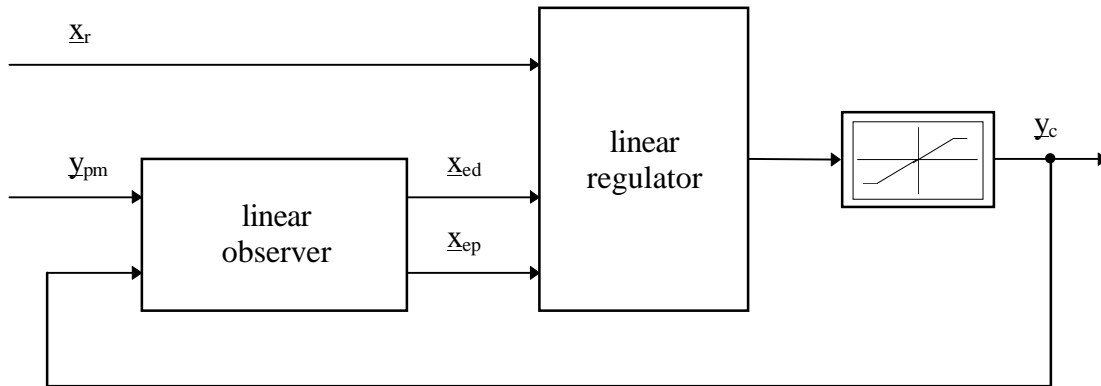


Fig. 6 Compensator with regulator and estimator

Since for implementation the reference model from the design structure will be replaced by a reference profile generator, the vector \underline{x}_r containing the load-side angular reference position, velocity and acceleration (see (2.2a)) becomes an input of the compensator. These signals will be derived from the corresponding reference signal for the linear carriage motion by division by the gear ratio i_s of the ball screw unit. The other inputs to the regulator are the estimates \underline{x}_{ed} of the disturbance model state and \underline{x}_{ep} of the plant state vector provided by the augmented plant observer subsystem implemented by equation (2.9). Since the disturbance input \underline{u}_d to the observer can not be measured, it has been omitted. As mentioned in the LQE design section, the observer has been designed robust for this. The saturation block before the compensator output and in the feedback to the observer control input is included to improve the state estimates when actuator saturations become effective in the plant control input path [14]. Its bounds are set equal to the servo amplifier maximum current limits so that the observer will get a correct input signal if the plant control input signal is saturated at these bounds. Due to the LTR design, the observer and thus the control system behave robust when the RMS current limits or the voltage limits are hit inside the amplifier. The regulator subsystem is assembled according to equation (2.4).

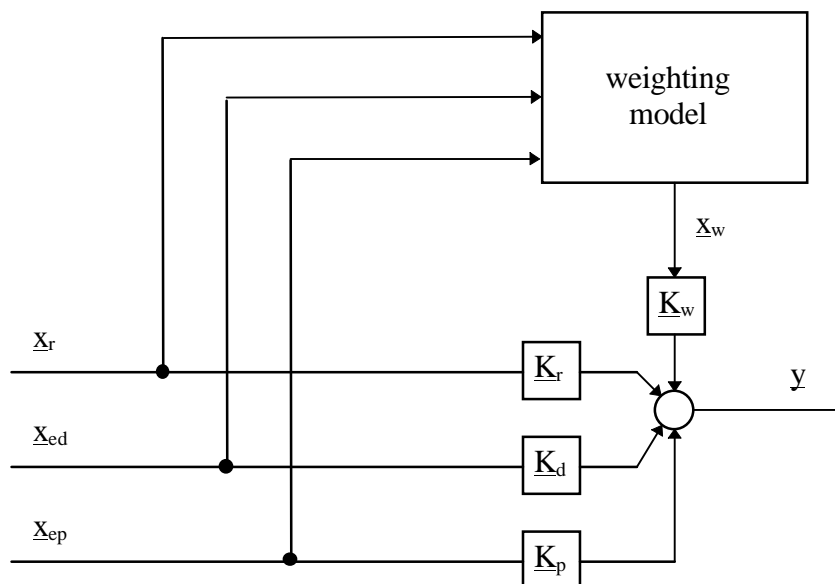


Fig. 7 Regulator with weighting model

If the weighting model in the augmented plant model for LQR design from figure 2 contributes a state \underline{x}_w , the corresponding dynamics

$$\dot{\underline{x}}_w = \underline{A}_w \underline{x}_w + \underline{B}_{wr} \underline{C}_r \underline{x}_r + \underline{B}_{wp} (\underline{C}_{po} \underline{x}_{ep} + \underline{D}_{pod} \underline{C}_d \underline{x}_{ed}) \quad (2.12a)$$

and their contribution to the regulator output

$$\underline{y}_{k_w} = \underline{K}_w \underline{x}_w \quad (2.12b)$$

will have to be added to the regulator block diagram. This would be the case for integral weighting with the model (2.2d). For purely proportional weighting with the model from equation (2.2c) which has been used for the regulator design the upper part of figure 7 has to be omitted.

The above compensator has been analyzed with the plant model for iterative fine tuning of the LQR/LQE design parameters to improve the final closed-loop system behaviour. One of the analysis steps is the assessment of the robustness of the linear control system by comparing the open-loop bode plots of the LQR and LQG controlled system for LTR. Figure 8 shows the LTR bode plots for the final compensator design. LTR has been nearly achieved.

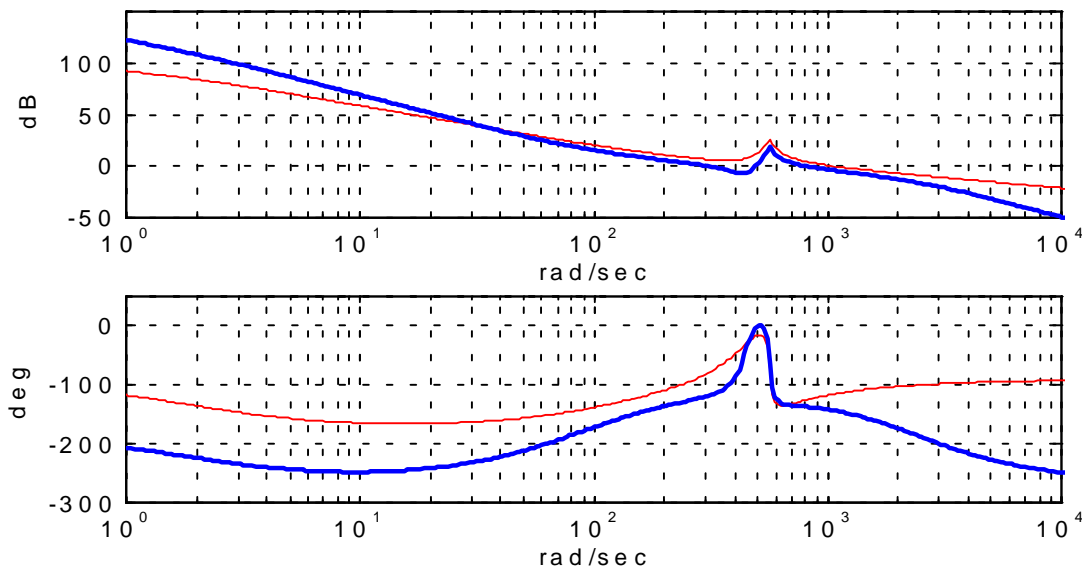


Fig. 8 *Open-loop bode plots for system with LQR (thin lines) and LQG compensator (bold lines)*

The robustness of the nonlinear control system against nonlinear plant characteristics like friction, saturations, tacho ripple and quantization, and against plant parameter variations has been checked by closed-loop simulation. As will be shown with the experimental results, this allowed a very good prediction of the real system behaviour.

3. Control implementation and results

Since the above compensator has been designed in the continuous time domain, its differential equations have to be discretized for an efficient digital implementation. A very straightforward option is to discretize the dynamic subsystems of the compensator, i.e. the weighting model in the regulator and the state space model of the observer, by using appropriate discretization methods. To check for the discretization and nonlinear implementation effects before starting with the real experiment, the discrete compensator has been closed-loop simulated with the continuous nonlinear plant model of the EMPS from section 1, including additional blocks for the signal interfaces. The corresponding SIMULINK block diagram is shown in figure 9. To correct for the offset and gain error in the real tachometer signal, a signal condition subsystem [15] had to be added to the control. The simulation results showed a remarkable robustness of the control system against process and measurement noise, and plant uncertainties, like a varying stiffness c_{dl} of the coupling between the drive and load side, a varying load-side inertia J_l and changing friction characteristic. A sampling rate of 4 kHz turned out to produce satisfying, quasi-continuous results. A simulation result for a small reference track is presented with the corresponding measurement in figure 12.

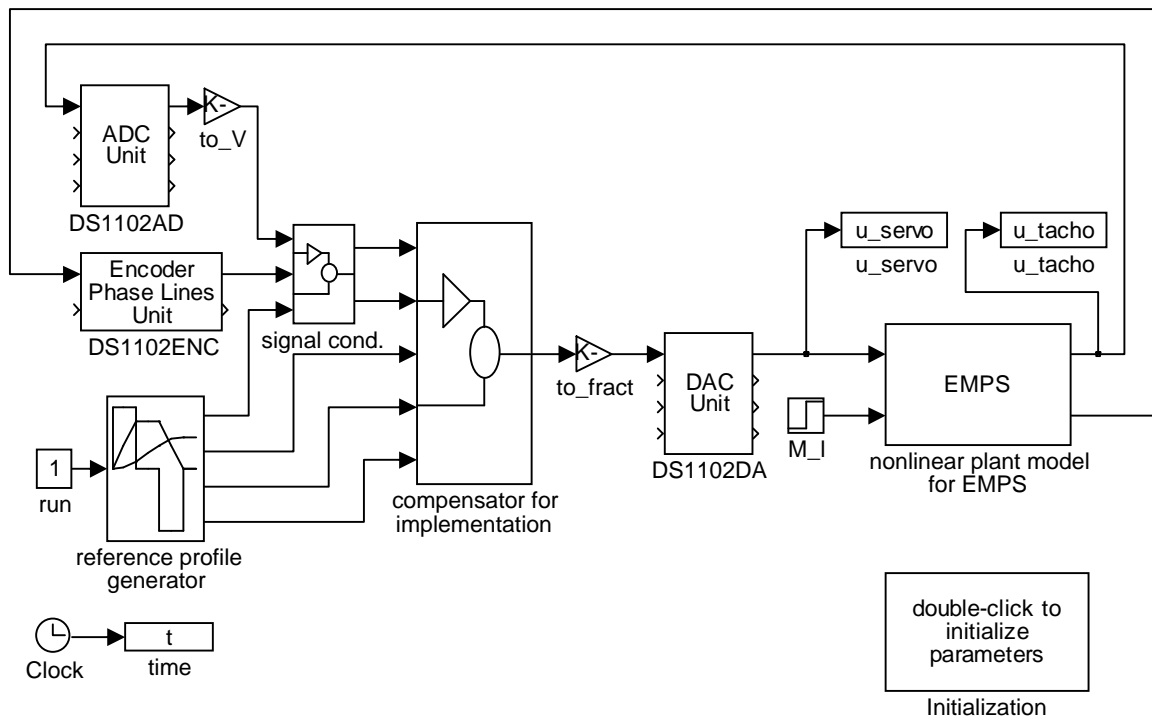


Fig. 9 Block diagram for nonlinear control system analysis by closed-loop simulation

For rapid prototyping the compensator, signal conditioning, reference profile generator and interfacing blocks from figure 9 have been copied to the block diagram in figure 10 which has been augmented by additional blocks for encoder index search (homing), operational and safety provisions. The used total development environment [3] allowed for a seamless transition to the experiment by automatic code generation, experiment control and data acquisition.

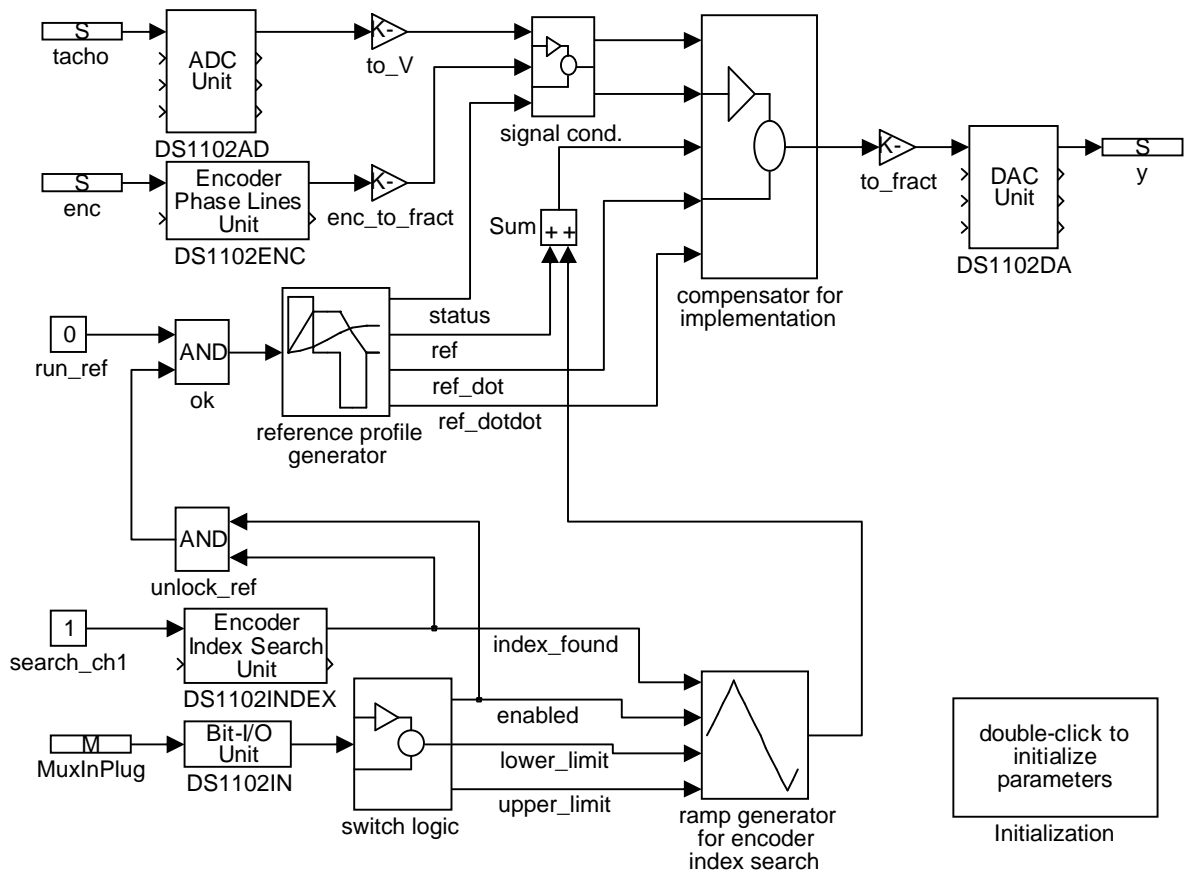


Fig. 10 Block diagram for control implementation by automatic code generation

An experimental result for the carriage reference motion from figure 11 commanded to the control is presented by the position error and control signal measurements in figure 12.

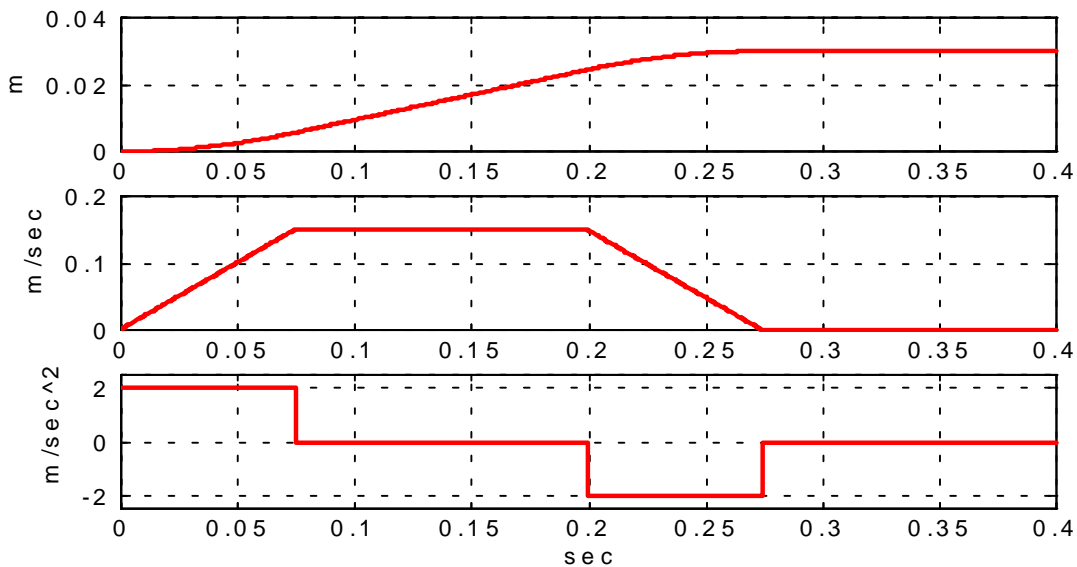


Fig. 11 Carriage reference position, velocity and acceleration from reference profile generator

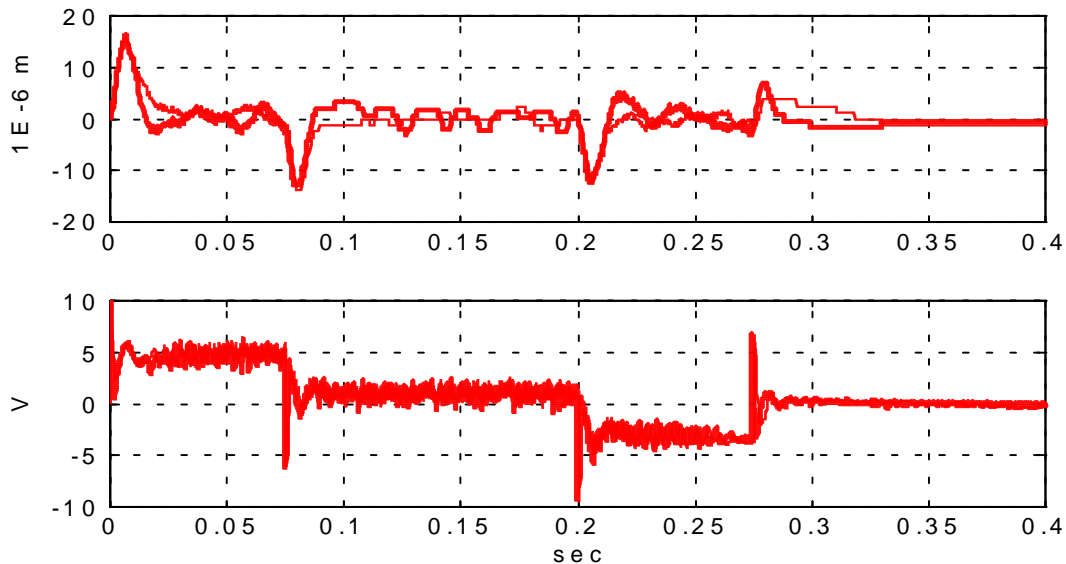


Fig. 12 Position error (top) and control signal (bottom) from measurement (bold line) and simulation (thin line)

The steps in the acceleration command produce a control signal close to the servo amplifier saturation bounds of $\pm 10V$. Despite this strong reference excitation, due to the high control bandwidth (see open-loop bode plots from figure 8), the maximum position error is less than $20 \mu m$ and the error settling times are about 10 msec. Vibrations from the flexible coupling between drive and load side are actively damped by the control. The control shows significantly better results than with the simpler compensator from [6], standard single-loop PID or P-PI cascade control [5]. Finally, the feedforward of the disturbance estimate from the observer and the high control bandwidth yields a strong rejection to external force or torque inputs F_1 or M_1 , which becomes evident in the experiment when one tries to twist the screw manually.

4. Conclusions

As shown for the EMPS, LQG control provides very good results in high speed and precise position control. This is achieved by a systematic approach in the control design including a modelling of the deterministic and stochastic reference and disturbance environment of the plant, and a modelling of the design objectives specified by the control engineer. The objective variables used in the LQR cost function, suitable weightings derived from the actual and desired variable bounds, and a rule to determine meaningful noise intensity matrices for the LQE design from sensor and signal interface specifications are crucial for a straightforward design procedure. Robustness of the linear control system with the resulting LQG compensator can be achieved by aspiring LTR with appropriate process noise intensities in the observer design. Further robustness analysis for the nonlinear control system and investigation of implementation effects have to be performed by simulation.

With the contemporary software tools for design and simulation the above systematic approach can be very well guided by design template files and a small graphical user interface [5]. A total development environment for rapid prototyping and experimentation allows for a seamless transition to the experiment and concept proving. With the knowledge of the basic theory one can easily develop advanced control concepts in a minimum of time. The LQG control design for the EMPS can be seen as a sample session for this.

References

- [1] B. Friedland, Control System Design. McGraw-Hill, 1986.
- [2] F. L. Lewis, Applied Optimal Control and Estimation. Prentice-Hall, Englewood Cliffs, NJ, USA, 1992.
- [3] H. Hanselmann, DSP in Control: The Total Development Environment. International Conference on Signal Processing Applications & Technology ICSPAT'95, Boston, MA, USA, October 24-26, 1996.
- [4] D. Weiske, Modellbildung für einen Positionierantrieb mit Reibung und Elastizität. Thesis for diploma degree at Cologne Laboratory of Mechatronics, FB KT, University of applied sciences Cologne, 1996.
- [5] H. Henrichfreise, Practical Issues on Classical and Modern Control of Electromechanical Drive Systems. Seminar at Conference PCIM'93, Nürnberg, Germany, June 21, 1993.
- [6] H. Henrichfreise, Observer based Coulombic friction torque compensation for a position control system. Proceedings of 21st Intelligent Motion Conference PCIM '92, Nürnberg, Germany, April 28-30, 1992.
- [7] R. Kasper, Entwicklung und Erprobung eines instrumentellen Verfahrens zum Entwurf von Mehrgrößenregelungen. Fortschritt-Berichte VDI, Reihe 8, Nr. 90, VDI-Verlag, Düsseldorf 1985.
- [8] J. Lückel and R. Kasper, Optimization of the disturbance and reference characteristics of linear, time-invariant systems by stationary compensation of unstable excitation models. Int. Journal of Control, No 41, 1985, pp. 259-269.
- [9] M. Wieland, Untersuchung des Einflusses einer dynamischen Bewertung der Entwurfszielgrößen beim LQR-Entwurf für eine Positionierregelung. Thesis for diploma degree at Cologne Laboratory of Mechatronics, FB KT, University of applied sciences Cologne, 1996.
- [10] A. Grace, A. J. Laub, J. N. Little and C. Thompson, Control System Tollbox User's Guide. The MathWorks, Inc., Natick, Mass. 01760, October 30, 1990.
- [11] A. J. Laub, A Schur Method for Solving Algebraic Riccati Equations. IEEE Trans. on Automatic Control, Vol. AC-24, 1979, pp. 913-921.
- [12] A. V. Oppenheim and R. W. Schaffer, Digital signal processing. Prentice-Hall, 1975.
- [13] J. C. Doyle and G. Stein, Robustness with Observers. IEEE Trans. on Automatic Control, Vol. AC-24, 1979, pp. 607-611.
- [14] H. Hanselmann, Implementation of Digital Controllers - A Survey. Automatica, Vol. 23, No. 1, 1987, pp. 7-32.
- [15] H. Henrichfreise and C. Witte, CAE-Supported Design and Testing of a Signalconditioning Subsystem for Analog Velocity Measurement in Position Control Applications. 7th German-Polish Seminar, University of applied sciences Cologne, May 8-14, 1995.